Available online at www.sciencedirect.com
SCIENCE DIRECT
Carbohydrate Polymers 65 (2006) 337–345
Carbohydrate Polymers
www.elsevier.com/locate/carbpol

Preparation of cholesterol-modified chitosan self-aggregated nanoparticles for delivery of drugs to ocular surface

Xu-bo Yuan [a,b], Hong Li [a,*], Yan-bo Yuan [c]

[a] *Institute of Polymer Chemistry, Nankai University, Tianjin 300071, China*
[b] *School of Materials Science and Engineering, Tianjin University, Tianjin 300072, China*
[c] *Changzhi medical college, Shanxi, Changzhi 046000, China*

Received 27 April 2005; received in revised form 10 January 2006; accepted 16 January 2006
Available online 22 May 2006

Abstract

Cholesterol hydrophobically modified chitosan (CS-CH) containing 1.7–4.7 cholesterol groups per 100 anhydroglucosamine units of chitosan were synthesized by an EDC-mediated coupling reaction. The physicochemical properties of the self-aggregated nanoparticles in physiological saline were studied using transmission electron microscopy, dynamic light scattering, and fluorescence spectroscopy. The mean diameters of all samples were less than 230 nm, and the critical aggregation concentration (CAC) of all self-aggregated nanoparticles in physiological saline less than 4.0×10^{-2} mg/ml. Both the mean diameters and the CAC decreased slightly with the increasing degree of substitution (DS) by hydrophobic groups. The self-aggregated CS-CH nanoparticles were radiolabeled by ^{99m}Tc, their ocular distribution was investigated using single photon emission computed tomography (SPECT) and scintillation counter. The CS-CH nanoparticles retained at the procorneal area, and no radioactivity was found in the posterior segment. The drug-loading and release behavior of the nanoparticles were investigated using Cyclosporine A (CyA) as the model drug. CyA was physically entrapped in the nanoparticles during the dialysis process, and the drug-loading ratio was 6.2%. A sustained release of CyA from CS-CH nanoparticles was observed. The results showed that CS-CH nanoparticles might represent an interesting vehicle to enhance the therapeutic index of clinically challenging drugs with potential application at extraocular level.

Keywords: Chitosan; Cholesterol; Hydrophobically modified; Self-aggregation; Ocular distribution; Drug release

1. Introduction

The therapy of extraocular diseases, such as keratoconjunctivitis sicca or dry eye disease, is limited by the short ocular residence time of drug on the ocular mucosa due to the rapid elimination from corneal surface by the lachrymal flow. To overcome, many studies are devoted to develop polymeric hydrogel systems to improve drugs ocular availability by increasing precorneal residence time (Bernatchez, Tabatabay, & Gurny, 1993; Ludwig, van Haeringen, Bodelier, & van Ooteghem, 1992; Unlü, van Ooteghem, & Hincal, 1992). Among the polymeric carriers used, cationic chitosan (CS) has attracted considerable attention due to its unique properties as good biocompatibility, biodegradability (Hirano, Seino, Akiyama, & Nonaka, 1990; Knapczyk, Kro'wczynski, Pawlik, & Liber, 1984) and the ability to enhance the paracellular transport of drugs (Artursson, Lindmark, Davis, & Illum, 1994). CS is a proposed material with a good application potentiality for ocular drug delivery. Its solution was found to considerably prolong the corneal residence time of antibiotic drugs (Felt et al., 1999). CS-coated nanocapsules were even more efficient in enhancing the intraocular penetration of some specific drugs (Calvo, Vila-Jato, & Alonso, 1997; Genta et al., 1997). Ionically crosslinked CS nanoparticles showed

* Corresponding author. Tel.: +86 22 23508388.
E-mail address: hongli@nankai.edu.cn (H. Li).

0144-8617/$ - see front matter © 2006 Elsevier Ltd. All rights reserved.
doi:10.1016/j.carbpol.2006.01.020

prolonged residence time at the ocular mucosa after topical administration to rabbits eyes (Angela, Alejandro, & María, 2001).

The nanoparticles prepared from amphiphilic chitosan have recently attracted increasing interest in pharmaceutical areas. Compared with the routine methods, such as covalently crosslinkage, ionically crosslinkage, and desolvation (Janes, Calvo, & Alonso, 2001), preparing nanoparticles through the self-assembly of amphiphilic CS is more simple and effective method, needing no additives. The nanoparticles size could be easily controlled by adjusting DS. Moreover, the hydrophobic microenvironments formed by the association of hydrophobic components enable the nanoparticles to act as a reservoir of hydrophobic drugs. Poly(ethylene glycol) (Ohya, Cai, Nishizawa, Hara, & Ouchi, 1999) palmitic acid (Uchegbu, Schatzlein, & Tetley, 1998) and deoxycholic acid (Lee, Kwon, & Kim, 1998) modified chitosan have been successfully used as carriers for control release of insulin, bleomycin, adriamycin, and DNA, respectively. Few reports till now, however, addressed the utilization of self-assembled systems of chitosan as the drug carriers for the therapy of ophthalmic diseases.

The purpose of the present work was to demonstrate the feasibility of amphiphilic chitosan self-aggragated nanoparticles as hydrophobic drug carrier. Cholesterol hydrophobic-modified chitosan (CS-CH) was synthesized, and its self-aggregates were prepared via diafiltration method. Physicochemical properties of the prepared nanoparticles were studied using transmission electron microscopy (TEM), dynamic light scattering (DLS), and fluorescence spectroscopy (FS). The ocular distribution of nanoparticles was investigated by SPECT and scintillation counter. The drug-loading of the nanoparticles was studied using Cyclosporine A (CyA) as the model drug, due to its hydrophobicity and well utilization in immunosuppression past corneal transplantation as well as the treatment of dry eye disease. CyA was physically entrapped in chitosan self-aggregates, and the control release behavior was investigated in vitro.

2. Experimental

2.1. Materials and animal

Chitosan samples were provided by the Nantong Suanglin Biochemical Co. Ltd. (China) with deacetylation degrees of 85 % and viscosity average molecular weight of 40 kDa. Cholesterol was purchased from Tianjin Chemical Reagent Co., China, and recrystallized in ethanol before use. 1-Ethyl-3-(3-dimethylaminopropyl) carbodiimide (EDC) was purchased from Sigma (St. Louis, MO). Pyrene as a fluorescence probe was purchased from Aldrich (St. Louis, MO). The physiological saline was medical grade, and the water was purified by distillation, deionization, and reverse osmosis (MilliQ Plus). New Zealand rabbits weighing between 2.0 and 2.5 kg were obtained from the Laboratory Animal Center of Academy Military Medical Sciences, China.

2.2. Synthesis of cholesterol 3-hemisuccinate

The synthesis of cholesterol 3-hemisuccinate (CHS) was carried out according to the procedure described by Kuhn, Schrader, Smith, and O'Malley (1975). One gram of succinic anhydride was added per gram of cholesterol and dissolved in 30 ml of pyridine. The mixture was stirred for 3 h at 70 °C. The crude product was dissolved in a minimum amount of H_2O/EtOH (1:10, v/v), and CHS was precipitated out from H_2O/MeOH (1:10, v/v), then recrystallized from EtOH.

2.3. Preparation of chitosan and cholesterol 3-hemisuccinate conjugates (CS-CH)

CS-CH was synthesized referring to the procedure described by Lee with minor modification (Lee et al., 1998). The typical procedure is as follows: CHS (0.34 mol/mol chitosan) in *N*,*N*-dimethyl formamide (DMF) was added to a 1% chitosan–hydrochloric acid solution followed by the dropwise addition of EDC (0.18 mol/mol CHS) under stirring at room temperature. After 24 h, the reaction mixture was poured into methanol/ammonia solution (7/3, v/v). The precipitates were filtered off, washed thoroughly with methanol, and a yellow gel was obtained. The gel was freeze-dried. The DS was controlled by varying the amount of CHS. The formation of the conjugate was confirmed by Fourier transform-infrared (FT-IR, Bio-Rad FTS 135) spectroscopy and ^{1}H NMR (Varian Unity plus 400) spectroscopy measurements. The DS, defined as the number of CHS groups per 100 anhydroglucosamine units of chitosan, was determined by elemental analysis.

2.4. Preparation of CS-CH self-aggregate

The self-aggregates of CS-CH were prepared by diafiltration methods. Fresh synthesized CS-CH gel was dissolved in 4 ml DMSO/water (7/3, v/v), and then the solution was dialyzed against physiological saline using the MWCO 14,000 g/mol dialysis membrane to form the polymeric aggregates. The medium was replaced every hour for the first 3 h period and every 3 h for the next 21 h. The resultant solution was poured into a dry 10-ml volumetric flask, and the flask was made up to the mark with physiological saline. To determine the concentration of the solution, equivalent amount of CHS gel was weighted, freeze-dried, and re-weighted accurately at the same time. The concentration of CHS solution ranges from 1 to 3 mg/ml.

The morphology of the polymeric aggregates was observed using a TEM (JEM-2000 FX II, Jeol, Japan). A drop of polymeric aggregates suspension was placed on a copper grid coated with carbon film and dried at 25 °C. Observation was performed at 80 kV. Size and size

distribution of polymeric aggregates were measured by Dynamic light scattering (DLS) (Brookhaven 90Plus/BI-MAS instrument with BI-9000 Goniometer) with a He–Ne laser beam at a wavelength of 658 nm at 25 °C and scattering angle of 90°. Meanwhile, the ζ-potential of the aggregate particles was measured using Powereach® (Zhongchen digital technology instrument Ltd., Shanghai China). All samples were sonicated for 3 min at 40 W with probe type sonifier for three times before every measurement.

2.5. Fluorescence spectroscopy measurement

To investigate the fluorescence spectroscopy characteristics, the CS-CH conjugate suspension was prepared in the same way as the aggregate preparation. The aggregate solution was adjusted to various CS-CH conjugate concentrations.

To prove the potential of hydrophobic microdomain formation and estimate the CAC of the CS-CH conjugate, the fluorescence spectroscopy was measured with a Spectrofluorophotometer (970CRT, Shanghai, China), using pyrene as a hydrophobic probe. Sample suspensions were prepared by adding a known amount of pyrene in acetone to a series of 20 ml vials, and then removing the acetone by evaporation to a final pyrene concentration of 6.0×10^{-7} M. Various concentrations (10 ml) of CS-CH conjugate suspension were then added to each vial and heated for 3 h at 65 °C to equilibrate the pyrene and the nanoparticles, and then remained undisturbed to cool overnight at room temperature. For the intensity ratio measurement of the first and the third highest energy bands in the emission spectra of pyrene, the slit openings for excitation and emission were set at 10 and 2 nm, respectively. The excitation wavelength (λ_{ex}) was 336 nm.

2.6. Radiolabeling of CS-CH aggregates and ocular-distribution

The radiolabeling of CS-CH aggregates was performed using the method reported by Banerjee, Mitra, and Singh (2002). Lyophilized CS-CH4.7 nanoparticles (2 mg/ml) were dispersed in Tris–HCl buffer (pH 7.2). Nitrogen purging, prior to mixing was carried out to degas all solutions. To 0.1 ml ^{99m}Tc (5.2 mCi) in saline, 5 mg of solid sodium borohydride was added directly with continuous stirring followed by immediate addition of the CS-CH nanoparticles buffer. The solution was stirred for 20 min at room temperature, then centrifugated at 18,000 rpm for 10 min followed by washing three times with buffer under sonication condition.

The ocular distribution of CS-CH aggregates was assessed by scintillation counter and single photon emission computed tomography (GE DISCOVERY-VH, USA) images analysis. After installation of 25 μl radiolabeled CS-CH aggregate solution onto the left cornea of rabbit, ocular dynamic SPECT imaging was immediately initiated. Two small plastic vial containing 0.5 ml radiolabeled CS-CH solution was placed perpendicularly or parallel to the rabbit eye as a orientation tracer (Fig. 7a). The SPECT images were collected at 0, 8, 22, 43, 71, and 112 min. The initial image was divided into five regions of interest, which were, respectively, (1) the position reference, (2) the precorneal surface (3) the posterior segment, (4) the lachrymal duct, and (5) the lacrimal sac.

The rabbits were killed after SPECT measurement. The eyes were proptosed and rinsed with physiological saline. Aqueous humor was withdrawn from the anterior chamber, and cornea, conjunctiva, and iris/ciliary body were subsequently dissected in situ. Each tissue was rinsed with physiological saline and weighted. The radioactivity of all samples was counted with scintillation counter.

2.7. Drug loading and in vitro drug release

To evaluate the CS-CH nanoparticles as drug carriers, CyA was incorporated as a hydrophobic model drug. The drug-loaded CS-CH nanoparticles were prepared by dialyzing the DMSO/water solution of CyA and CS-CH against physiological saline. The drug loading content was calculated as the ratio of the weight of drug entrapped in the nanoparticles with that of nanoparticles.

In vitro drug release was preformed in the physiological saline. Five milligrams of CyA-loaded nanoparticles and 1 ml saline were placed in a dialysis membrane (MWCO 2000 g mol^{-1}). Then the dialysis membrane was introduced into a vial with the same saline (10 ml), and the media were stirred at 37 °C and 75 rpm. At predetermined time intervals, the entire medium was removed and replaced with the same amount of fresh saline. The amount of CyA released from nanoparticles was determined by UV spectrophotometer at 214 nm.

3. Results and discussion

3.1. Synthesis

The conjugation scheme of chitosan with CHS (Fig. 1) was confirmed by analysis of FT-IR and ^{1}H NMR. Fig. 2 shows the FT-IR spectra of chitosan (a) and CS-CH conjugate (b). The absorption band at 1650 cm^{-1} was attributed to the carbonyl of O=C-NHR of chitosan (Osman & Arof, 2003). And the absorption band at 1599 cm^{-1} was assigned to the amino groups of chitosan with high deacetylation degrees. This signal shifted to 1528 cm^{-1} after the conjugation reaction, indicating the formation of new amide bonds by acylation of amino groups of chitosan with activated carboxyl groups of CHS. A weak shoulder peak occurred at 1738 cm^{-1} assigned to the carbonyl of ester bond of CHS, further confirming the conjugation of CHS to chitosan.

The incorporation of CHS to the chitosan was also confirmed by ^{1}H NMR spectroscopy and the result was shown in Fig. 3. Although the signals of chitosan were overlapped by that of deuterated DMSO solvent, the characteristic

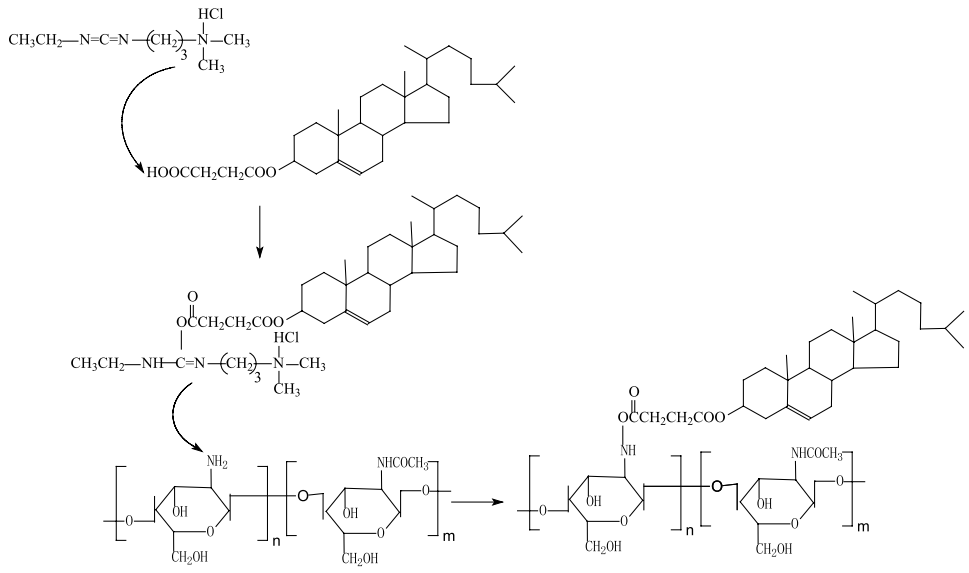

Fig. 1. The scheme of conjugation of chitosan and cholesterol-hemisuccinate.

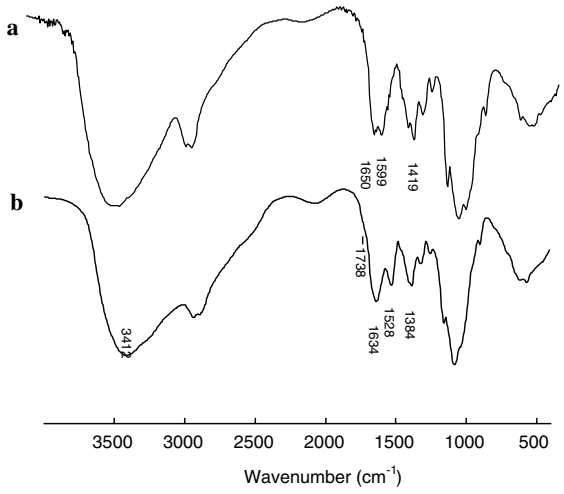

Fig. 2. IR spectra of (a) chitosan, (b) CS-CH4.7

resonances assigned to the angular methyl groups on carbon 18 and 19 and the methyl groups on carbons 21, 26, and 27 of cholesterol at 0.6–1.0 ppm were clearly observed (Birgit, James, & Rawle, 1998). The results evidenced that the modified chitosan contained cholesterol residues. The DS of the chitosan derivative was calculated from the elemental analysis data, and the result was list in Table 1. The number behind the sample code CS-CH in Table 1 indicates the DS of the sample. It can be seen from Table 1 that DS increased as the concentration of CHS and EDC increased, and the DS is in the range from 1.7 to 4.7 per 100 anhydroglucosamine units of chitosan.

3.2. Self-aggregation of CS-CH

The self-aggregates of amphiphilic polysaccharides can be prepared through sonication or diafiltration methods. As for sonication, modified polysaccharides were suspended in deionized water or phosphate-buffered saline solution followed by sonication to form optical clear solution. While in the case of diafiltration, the polysaccharides were dissolved in co-solvent and then dialyzed against water. In the present study, we found the CS-CH was hardly dissolved in organic solvents (even DMSO) or their mixture with water after freeze-drying, and neither optical clear solution nor nanoparticles regularized in shape could be formed by sonication. So fresh synthesized CS-CH gel was employed to prepared self-aggregates and the concentrations of the solution were determined via weighing of equivalent amount of gel after freeze-drying (as described in Section 2).

The structure and self-aggregate behavior of CS-CH were investigated by TEM, DLS, and FS. Fig. 4 shows the TEM photographs (left) and histograms of the size distribution (right) of the CS-CH measured by DLS. The shapes of CS-CH nanoparticles observed were mostly spherical, and the diameters of the nanoparticles were 50–200 nm. It can be found from the micrographs that the nanoparticles formed by CS-CH with various DS values possess different microstructure. The nano-spheres composed of CS-CH1.7 were homogeneous in structure, and the histogram of size distribution showed one peak centered at 228 nm. The nano-spheres of CS-CH4.7, however, seem to made up of small particles whose diameters were round 10–30 nm, and two peaks centered at 56 and 216 nm could be seen in their size distribution histogram. The results of TEM and DLS imply that the DS values show great effect on the aggregation of CS-CH. In the case of low DS, the intramolecular association is weak probably due to the relatively large persistence length of the chitosan chain. Consequently, the CS-CH micelles formed through intermolecular interaction predominantly, and the micelles are loose primary aggregates swelled by water. As the DS increased, the intramolecular association of cholesterol

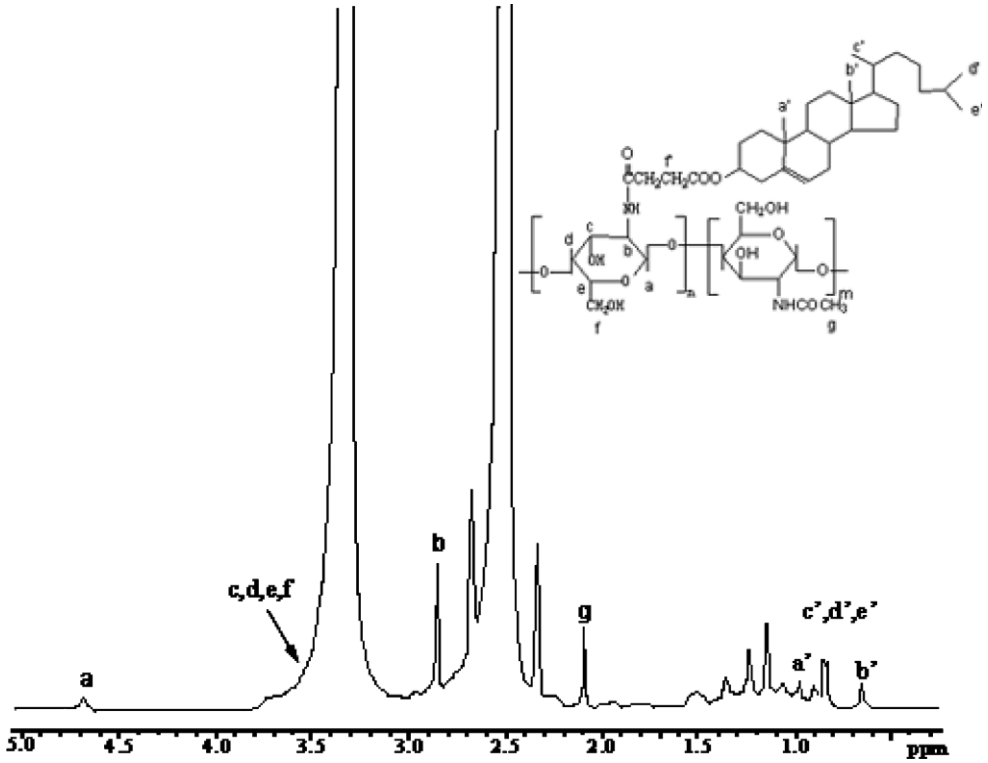

Fig. 3. ^{1}H NMR spectrum of CS-CH4.7 conjugate (in deuterated DMSO).

Table 1
Properties of cholesterol-modified chitosan

Sample	Molar ratio of Uagl:CHS [a]	DS[b]	CAC[c] ($\times 10^{-2}$ mg/ml)	Mean diameter[d] (nm)	Variance[d]	ζ-potential
CS-CH1.7	100/10	1.7	3.85	226.1	0.126	44.60
CS-CH2.7	100/21	3.7	2.04	219.6	0.120	44.88
CS-CH4.3	100/30	4.3	1.82	217.8	0.128	44.31
CS-CH4.7	100/38	4.7	1.35	185.2	0.153	43.14

[a] Anhydroglucosamine units of chitosan.
[b] DS of CHS per 100 anhydroglucosamine units of chitosan measured by elemental analysis.
[c] Determined by fluorescence spectroscopy.
[d] Effective diameter and variance determined by dynamic light scattering.

groups was enhanced, the polymer chains trend to compact coil, leading to the formation of small and very compact aggregates. The second aggregate appeared in the solution indicates the strong inter-particles interaction between self-aggregates.

The aggregation behavior of CS-CH in aqueous media was monitored by fluorometry in the presence of pyrene as a fluorescence probe. Fig. 5 shows the fluorescence emission spectra of pyrene incorporated into self-aggregates of CS-CH4.7 in physiological saline at 25 °C. If micelles or other hydrophobic microdomains are formed in an aqueous solution, the pyrene preferably lies close to (or inside) these microdomains and strongly emits, while it is quenched in polar media (Magny, Iliopolous, Zana, & Audebert, 1994). When the pyrene coexists with CS-CH4.7 self-aggregates, the total emission intensity increases and especially the intensity of the third highest vibrational band at 383 nm (I_3) starts to increase drastically at a certain concentration of polymeric amphiphiles. This concentration is defined as CAC, which means the threshold concentration of self-aggregation of polymeric amphiphiles.

The CAC can be determined by measuring the intensity ratio (I_1/I_3) of the first (372 nm) and the third highest energy bands in the emission spectra of pyrene. The variation of the intensity ratio (I_1/I_3) is shown in Fig. 6. At low concentrations of polymeric amphiphiles, the I_1/I_3 values are close to the value (1.87) for pyrene in water (Lee & Jo, 1998) followed by a linear decrease with the addition of polymeric amphiphiles above CAC. The CAC is determined by the interception of two straight lines. The CAC values of CS-CH (Table 1) are 0.01–0.04 mg/ml, which were much lower than the critical micelle concentration (cmc) of low molecular weight surfactants, indicating the stability of self-aggregates at dilute conditions. From Table 1 it can also be seen that the increase of hydrophobicity by

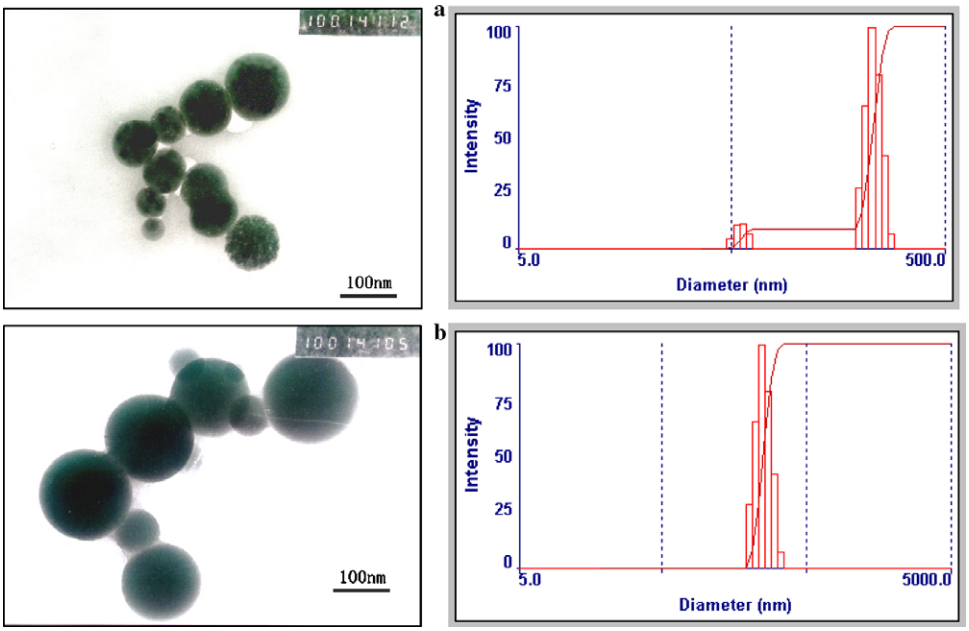

Fig. 4. TEM micrographs and size distribution of CS-CH self-aggregates measured using DLS. (The magnifying ratio of micrographs is 100K, and the scale bar = 100 nm was added by author. (a) CS-CH4.7, concentration = 1.4 mg/ml. (b) CS-CH1.7, concentration = 2.0 mg/ml.)

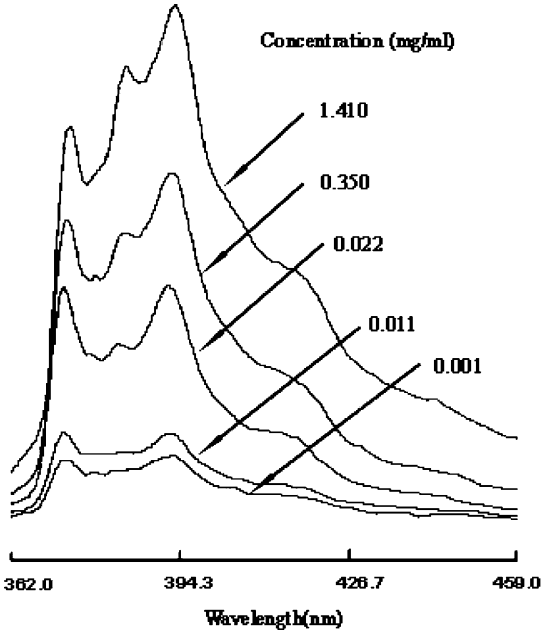

Fig. 5. Fluorescence emission spectra of pyrene (6×10^{-7} M) as a function of CS-CH4.7 concentration (excitation wavelength, 336 nm).

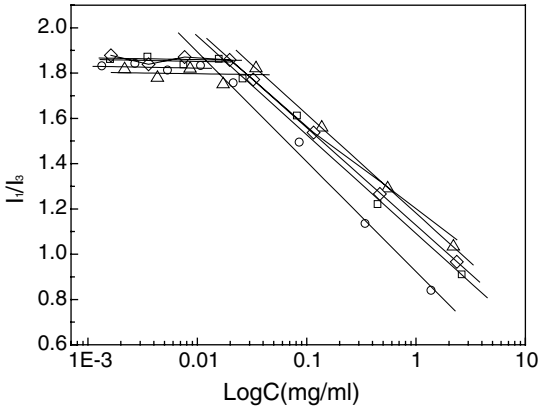

Fig. 6. Intensity ratio (I_1/I_3) for pyrene in physiological saline as a function of CS-CH concentration. (○) CS-CH4.7; (□) CS-CH4.3; (◇) CS-CH3.7; (△) CS-CH1.7.

introduction of a large amount of hydrophobic groups reduces the CAC values, and the mean diameters were reduced as DS increased though the size distribution was not monodisperse due to the presence of small primary and large secondary aggregates.

The ζ-potential of the Chol-CS nanoparticles seems scarcely influenced by the DS values. The reason might due to, on the on hand, the low degree of substitute, and one the other hand, the hydrophobic components aggregated inside the particles such the charge of nanoparticles was controlled mainly by the polysaccharide exposed to surface.

3.3. The ocular distribution of CS-CH self-aggregates

The observation of the acquired gamma-camera images was showed in Fig. 7. The CS-CH nanoparticles showed a good spreading over the entire precorneal area immediately after the topical administration, then part of the suspensions drained into lachrymal duct and from there, get into the lacrimal sac. These parts of suspensions were eliminated rapidly in the following 15 min, leaving 72.4% of ^{99m}Tc radiolabeled CS-CH aggregates stayed at the ocular surface. The remaining activity at 22, 43, 71, and 112 min were 72.4%, 72.0%, 71.9%, and 71.4%, respectively, indicating the well retention ability of CS-CH aggregate at the procorneal area.

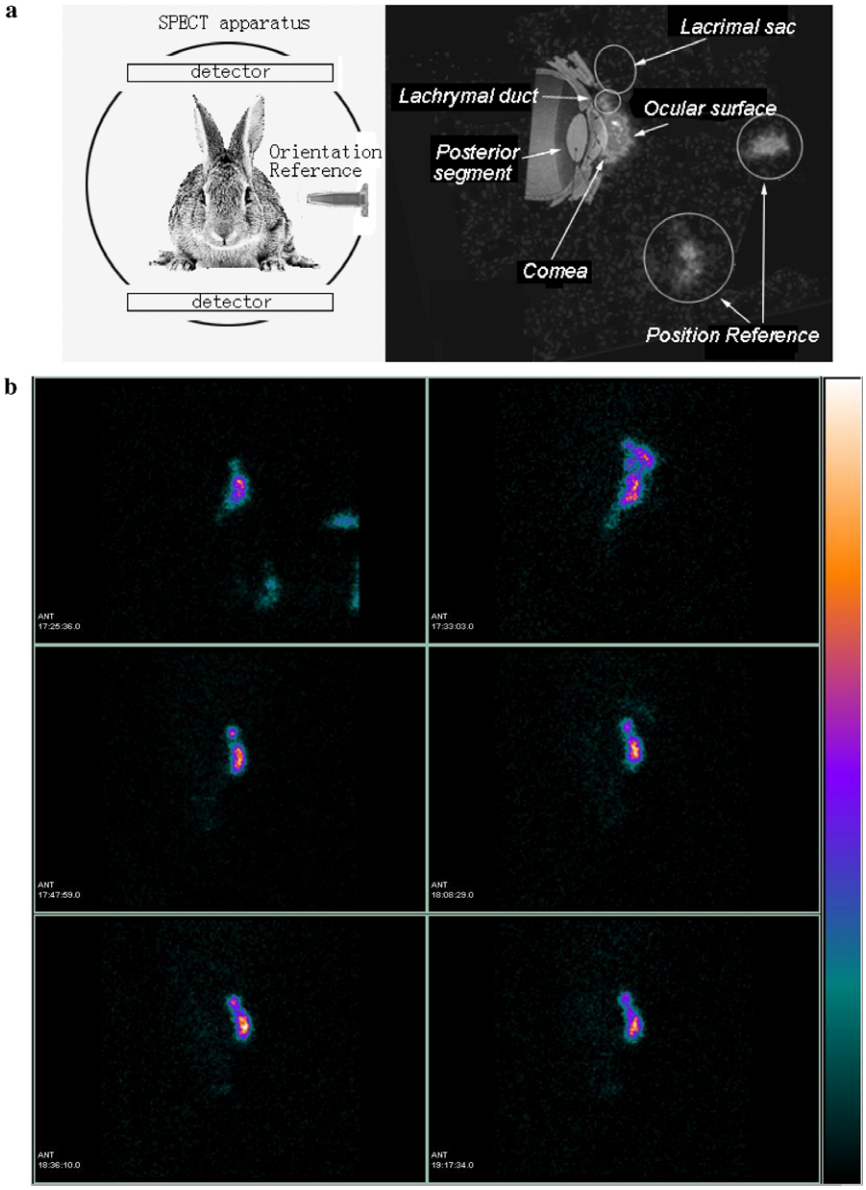

Fig. 7. Ocular distribution of CS-CH4.7 aggregates (measured by SPECT, (a) illustration for SPECT measurement and the orientation of the section of rabbit eye, (b) the ocular-distribution of CS-CH aggregates at different time).

The good residence time of chitosan and its nanoparticles at the ocular surface is ascribed to the bioadhesion ability based on its cationic activation (He, Davis, & Illum, 1998; Henriksen, Green, Smart, Smistad, & Karlsen, 1996; Lehr, Bouwstra, Schacht, & Junginger, 1992). In fact, this ability enables chitosan to open the tight junctions and in this way allows paracellular transport across the epithelium. Both nasal and oral drug delivery researches have demonstrated that significantly higher amounts of macromolecular drugs can be transported by co-administration with chitosan (Artursson et al., 1994; Illum, Farraj, & Davis, 1994; Kotzé et al., 1997). The cornea is the clear portion of the eye located right out front. It is just like a sandwich in which the outside is epithelium. But we did not find any obvious permeation of CS-CH aggregate through cornea into the posterior segment as indicated in Fig. 7 and the result of scintillation counter measurement (Table 2), even though the ζ-potential of the CS-CH aggregate nanoparticles measured by BI-zeta plus reaches about 44 mV. From Table 2 it can be seen that most of

Table 2
The relative radioactivity of CS-CH aggregates at different parts of rabbit eye

Portion of the eye	Cornea	Conjunctiva	Iris/ciliary body	Aqueous humor	Blood
Relative radioactivity (%)	78.3	20.1	0.7	0.2	0.2

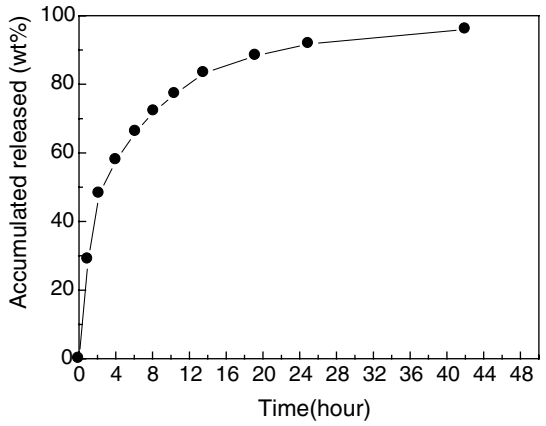

Fig. 8. CyA release from CS-CH self-aggregated nanoparticles (in physiological saline, 37 °C).

the radio-labeled CS-CH aggregates stayed at cornea and conjunctiva, and very few of aggregates permeate into iris/ciliary body. The radio activity of the aqueous humor and blood is so low that near to the radio activity of background. The poor permeation of CS-CH aggregates may be ascribed to the multi-layer structure of cornea. The corneal tissue is arranged in five basic layers, i.e., epithelium, Bowman's Layer, stroma, Descemet's membrane, and endothelium. The complex structure hinders the transport of CS-CH nanoparticles.

3.4. Drug loading and in vitro drug release

The maximum loading of CyA reached 6.2% of the CS-CH self-aggregated nanoparticles, suggesting a loading efficiency of 41.8%. Fig. 8 showed the in vitro release profiles of CyA from nanoparticles in saline. The CyA appeared to be released in a biphasic way, which characterized by an initial release or rapid release period followed by a step of slower release. The burst effect was observed in 4 h, in which 60% of the initial drug was released from nanoparticles. After this initial effect, CyA was released in a continuous way for up to 48 h, reaching percentage of cumulative release close to 95%.

4. Conclusions

A series of amphiphilic conjugates of chitosan and cholesterol 3-hemisuccinate were synthesized using 1-ethyl-3-(3-dimethylaminopropyl) carbodiimide as catalyst. The chemical structure of the conjugate was characterized by FTIR and ^{1}H NMR. The degree of substitution measured by elemental analysis were 1.7–4.7 cholesterol groups/100 anhydroglucosamine units of chitosan. The self-aggregate behavior of the conjugates was investigated by fluorescence spectrum, TEM, and DLS. The results showed that the CS-CH can form self-aggregate nanoparticles with hydrophobic inner core in physiology saline, and the critical aggregate concentration of the conjugates was about $1.35–3.85 \times 10^{-2}$ mg/ml defined by the degree of substitute. The self-aggregate nanoparticles of CS-CH were radiolabeled by ^{99m}Tc, and their ocular distribution was studied by SPECT and scintillation counter. CS-CH nanoparticles show good retention ability at the procorneal area, and no radioactivity was found in the posterior segment. Hydrophobic drug CyA was entrapped in the nanoparticles successfully using simple dialysis method, and the drug-loading content reached about 6%. A sustained release of CyA from CS-CH nanoparticles was observed over 48 h, indicating that the CS-CH aggregates can be a potential carrier of hydrophobic drug for the treatment of external ocular diseases.

Acknowledgments

This project was financially supported by the National Nature Science Foundation of China (Grant No: 50301008), National Basic Science Research Program (973 project, Grant No: 2002CCA02500), and the Innovation Foundation of Nankai University, China.

References

Angela, M. D. C., Alejandro, S., & María, J. A. (2001). Chitosan nanoparticles: a new vehicle for the improvement of the delivery of drugs to the ocular surface. Application to cyclosporin A. *International Journal of Pharmaceutics, 224*, 159–168.

Artursson, P., Lindmark, T., Davis, S. S., & Illum, L. (1994). Effect of chitosan on the permeability of monolayers of intestinal epithelial cells (Caco-2). *Pharmecutical Research, 11*, 1358–1361.

Banerjee, T., Mitra, S., & Singh, A. K. (2002). Preparation, characterization and biodistribution of ultrafine chitosan nanoparticles. *International Journal of Pharmaceutics, 243*, 93–105.

Bernatchez, S. F., Tabatabay, C., & Gurny, R. (1993). Sodium hyaluronate 0.25% used as vehicle increases the bioavailability of topically administered gentamicin. *Graefe's Archives for Clinical and Experimental Ophthalmology, 231*, 157–171.

Birgit, Z., James, J. B., & Rawle, I. (1998). Cholesterol and its derivatives, are the principal steroids isolated from the leech species *Hirudo medicinalis*. *Comparative Biochemistry and Physiology Part C, 120*, 269–282.

Calvo, P., Vila-Jato, J. L., & Alonso, M. J. (1997). Evaluation of cationic polymer-coated nanocapsules as ocular drug carriers. *International Journal of Pharmaceutics, 53*, 41–50.

Felt, O., Furrer, P., Mayer, J. M., Plazonnet, B., Buri, P., & Gurny, R. (1999). Topical use of chitosan in ophthalmology: Tolerance assessment and evaluation of precorneal retention. *International Journal of Pharmaceutics, 180*, 185–193.

Genta, I., Conti, B., Perugini, P., Pavaneto, F., Spadaro, A., & Puglisi, G. (1997). Bioadhesive microspheres for ophthalmic administration of acyclovir. *The Journal of Pharmacy and Pharmacology, 49*, 737–742.

He, P., Davis, S. S., & Illum, L. (1998). In vitro evaluation of the mucoadhesive properties of chitosan microspheres. *International Journal of Pharmaceutics, 166*, 75–88.

Henriksen, I., Green, K. L., Smart, J. D., Smistad, G., & Karlsen, J. (1996). Bioadhesion of hydrated chitosans: An in vitro and in vivo study. *International Journal of Pharmaceutics, 145*, 231–240.

Hirano, S., Seino, H., Akiyama, Y., & Nonaka, I. (1990). Chitosan: a biocompatible material for oral and intravenous administrations. In *Progress in Biomedical Polymers*. New York: Plenum, pp. 283–290.

Illum, L., Farraj, N. F., & Davis, S. S. (1994). Chitosan as a novel nasal delivery system for peptide drugs. *Pharmaceutical Research, 11*, 186–1190.

Janes, K. A., Calvo, P., & Alonso, M. J. (2001). Polysaccharide colloidal particles as delivery systems for macromolecules. *Advanced Drug Delivery Reviews, 47*, 83–97.

Knapczyk, J., Kro'wczynski, L., Pawlik, B., & Liber, Z. (1984). Pharmaceutical dosage forms with chitosan. In *Chitin and chitosan: Sources, chemistry, biochemistry, physical properties and applications*. London: Elsevier, pp. 665–669.

Kotzé, A. F., Luessen, H. L., De Leeuw, B. J., De Boer, A. G., Verhoef, J. C., & Junginger, H. E. (1997). *N*-Trimethyl chitosan chloride as a potential absorption enhancer across mucosal surfaces: in vitro evaluation in intestinal epithelial cells (Caco-2). *Pharmaceutical Research, 14*, 1197–1202.

Kuhn, R. W., Schrader, W. T., Smith, R. G., & O'Malley, B. W. (1975). Progesterone binding components of chick oviduct. *Journal of Biological Chemistry, 250*, 4220–4228.

Lee, K. Y., Kwon, I. C., Kim, Y. H., et al. (1998). Preparation of chitosan self-aggregates as a gene delivery system. *Journal of Controlled Release, 51*, 213–220.

Lee, K. Y., & Jo, W. H. (1998). Physicochemical characteristics of self-aggregates of hydrophobically modified chitosans. *Langmuir, 14*, 2329–2332.

Lehr, C. M., Bouwstra, J. A., Schacht, E. H., & Junginger, H. E. (1992). In vitro evaluation of mucoadhesive properties of chitosan and some other natural polymers. *International Journal of Pharmaceutics, 78*, 43–48.

Ludwig, A., van Haeringen, N. J., Bodelier, V. M. W., & van Ooteghem, M. (1992). Relationship between precorneal retention of viscous eye drops and tear fluid composition. *International Ophthalmology, 16*, 23–26.

Magny, B., Iliopolous, I., Zana, R., & Audebert, R. (1994). Mixed micelles formed by cationic surfactants and anionic hydrophobically modified polyelectrolytes. *Langmuir, 10*(9), 3180–3187.

Ohya, Y., Cai, R., Nishizawa, H., Hara, K., & Ouchi, T. (1999). Preparation of PEG-grafted chitosan nano-particle for peptide drug carrier. *Proceedings of the International Symposium on Controlled Release on Bioactive Materials, 26*, 655–656.

Osman, Z., & Arof, A. K. (2003). FTIR studies of chitosan acetate based polymer electrolytes. *Electrochimica Acta, 48*, 993–999.

Uchegbu, I. F., Schatzlein, A. G., & Tetley, L. (1998). Polymeric chitosan-based vesicles for drug delivery. *Journal of Pharmacy and Pharmacology, 50*, 453–458.

Unlü, N., van Ooteghem, M., & Hincal, A. A. (1992). A comparative rheological study on Carbopol viscous solutions and, the evaluation of their suitability as the ophthalmic vehicles and artificial tears. *Pharmaceutica Acta Helvetiae, 67*, 5–10.